

# Heat transfer through porous solids with complex internal geometries

D. A. ZUMBRUNNEN, R. VISKANTA and F. P. INCROPERA  
Heat Transfer Laboratory, School of Mechanical Engineering, Purdue University,  
West Lafayette, IN 47907, U.S.A.

(Received 8 January 1985 and in final form 27 August 1985)

**Abstract**—A thermal conductance model for heat transfer in a porous solid has been developed by using a probabilistically determined unit cell for a characteristic geometry. An apparatus was designed and used to measure overall thermal conductances (effective thermal conductivities) of several porous solids over a wide temperature range. A parameter required by the model was inferred from the measurements, and predicted and measured overall thermal conductances agreed to within the uncertainty of the experiments. Parametric calculations indicate that, when radiation is significant, overall thermal conductance increases with the temperature difference across the porous solid and is independent of thickness when the thickness is large relative to the pore size.

## 1. INTRODUCTION

RELATIVELY little attention has been given to the influence of temperature difference and thickness on the overall thermal conductance (or 'effective thermal conductivity') of porous solids. Current theoretical thermal conductance models are often restricted to small porosity ranges or require detailed information about the geometries of internal structures. However, many porous solids contain nonuniformly distributed pores with complex geometries. Examples include commercial products such as firebricks, ceramics and insulations, as well as naturally occurring porous solids such as rocks and residue materials.

The transport of heat in porous solids can occur by the combined mechanisms of conduction, convection and radiation. Typically, their cumulative effect is represented by an overall thermal conductance which is analogous to the thermal conductivity of the Fourier-Biot law. Overall thermal conductance generally differs from the local thermal conductance  $K$ , which depends on local temperature. Overall thermal conductances can be measured experimentally or can be determined by solving a one-dimensional energy equation which uses the Fourier-Biot law with model-generated local thermal conductances. Experimental methods are often in accordance with, or related to, standard test methods of the American Society for Testing and Materials (ASTM) [1]. In these methods, overall thermal conductances are determined for various average temperatures and are assumed to be generally applicable to all thicknesses and overall temperature differences. However, research regarding fibrous insulation [2, 3] has suggested that overall thermal conductance may not depend on average temperature alone, if the thermal radiation contribution to heat transfer is important. Francl and Kingery [4] have shown that thermal radiation can contribute significantly to heat transfer in porous solids. Accordingly,

the current practice which regards overall thermal conductance measurements of porous solids as simple property measurements, dependent only on average temperature, should be reconsidered.

Many theoretical models are based on a unit cell. A physical geometry, which is replicated everywhere in a porous system, is idealized and represented by a characteristic geometry. The local thermal conductance is determined by formulating and combining thermal resistances for each heat transfer mechanism associated with the unit cell. Unfortunately, the physical geometries of many porous solids can not be easily idealized and unit cell models of porous solids have had only limited success.

The widely used unit cell model of Loeb [5] is not applicable to many porous solids, since heat transfer by conduction through the fluid in the pores is ignored. Saegusa *et al.* [6] utilized a unit cell model consisting of a finite right-circular cylinder which contained a spherical pore. The model assumes that all pores are spherical even though many porous solids contain irregularly shaped pores and the porosity can not exceed 52%. Heat transfer occurred in the direction perpendicular to the circular faces of the cylinder, and the thermal conductance was determined from the temperature distribution in the cylinder. Whitaker [7] formulated equations for total energy transport in porous media by spatially averaging pertinent parameters. However, because the precise geometry of the medium must be specified when using the model, it is impractical for many porous solids. Maxwell [8] derived an expression for the effective electrical conductivity for current flow in a composite material containing a spherical dispersed phase within a larger sphere of a continuous phase. Chiew and Glandt [9] utilized this expression to determine the thermal conductances of porous media by introducing a 'radiation conductivity' to enhance transport across the gas in a pore. Their model is only valid at low porosities, however, since Maxwell

## NOMENCLATURE

$A$	cross-sectional area in the direction of heat transfer	$x$	distance along the direction of heat transfer in the characteristic geometry for the thermal conductance model.
$k_e$	overall thermal conductance of a sample defined by equation (11)	Greek symbols	
$k_f$	thermal conductivity of fluid in pores	$\beta$	$v/s$
$k_s$	thermal conductivity of solid	$\varepsilon$	total hemispherical emissivity of material at the surface of a pore
$K$	local thermal conductance	$\xi$	nondimensional space coordinate, $x/L$
$l$	effective length for conduction across pores	$\zeta$	parameter governing the importance of heat transfer through solid in a porous solid, equation (9)
$L$	material sample thickness	$\theta$	dimensionless temperature, $(T - T_C)/(T_H - T_C)$
$p$	porosity expressed in decimal form	$\Lambda$	average number of pores contained in path II of the thermal conductance model, see Fig. 2
$q$	total heat flux	$v$	dimensionless parameter, $4\varepsilon\sigma v T^3/k_s$
$q_R$	radiation heat flux	$\sigma$	Stefan-Boltzmann constant
$R$	thermal resistance	$\phi$	$l/v$
$s$	characteristic pore spacing in a porous solid	$\psi$	parameter in thermal conductance model which is unity if pores are closed and zero if pores are interconnecting.
$t$	length of a unit cell		
$T$	temperature		
$\bar{T}$	average temperature of the surface of a pore		
$T_{ave}$	average temperature of a sample, $(T_H + T_C)/2$		
$T_C$	cooled surface temperature of a sample		
$T_H$	heated surface temperature of a sample		
$v$	characteristic size of pores in a porous solid		

assumed that sphere separation was sufficient to preclude mutual interactions. In fact, Turner [10] noted that Maxwell's expression does not provide the same result when the conductivities of the phases are interchanged.

For the porous solids of this study and in many engineering applications, it is not practical to incorporate details of the complex pore geometry within a thermal conductance model. However, many important characteristics of these porous media can be determined probabilistically to form simpler characteristic geometries which are representative of the porous media. These characteristic geometries can be used to formulate thermal conductance models which include the pertinent heat transfer modes.

To determine whether parameters other than average temperature affect overall thermal conductance and to interpret and correlate the experimental results, a new thermal resistance model for which a unit cell is determined probabilistically has been developed. The model is applicable over a wide porosity range and does not require a detailed description of the geometry of the porous system. With a single empirical factor included in the model, calculated overall thermal conductances are in good agreement with experimental results.

## 2. EXPERIMENTAL METHODS

### 2.1. Test apparatus

The test cell used in this study (Fig. 1) resembles the ASTM-approved apparatus for measuring the overall

thermal conductances of firebricks and refractories and is a derivative of the cell employed by Fetters *et al.* [11]. Heat from an electric furnace passes through a porous solid, which is supported by a thin metallic substrate plate, and is then transferred across a narrow air space to a water-cooled copper calorimeter. In the ASTM-approved method, the test specimen rests directly on the calorimeter, while in the test cell of Fig. 1, direct contact is not made and more uniform cooling is provided to the sample. The combined resistances of the air space and test specimen decrease the heat transfer rate to the calorimeter, reducing furnace power requirements.

Side and bottom thermal guards are incorporated as a single, integral unit which resembles a shallow rectangular trough. Heat is transferred from the sidewalls of the trough by conduction to the base region. Since the sidewalls are cooled only by conduction, the temperature of the base remains below that of the sidewalls when the sidewall and calorimeter temperatures are equal, thereby eliminating natural circulation in the air space between the calorimeter and guard.

Three quartz spacers support the substrate plate and sample. Each spacer has a pyramidal shape to diminish perturbations in the temperatures of the substrate plate and calorimeter. Four cubical quartz blocks, which rest on the floor of the furnace cavity, were used to support the integral guard. Insulation was placed between the integral guard and furnace floor to reduce heat transfer to the guard. Firebrick was used to enclose the test cell

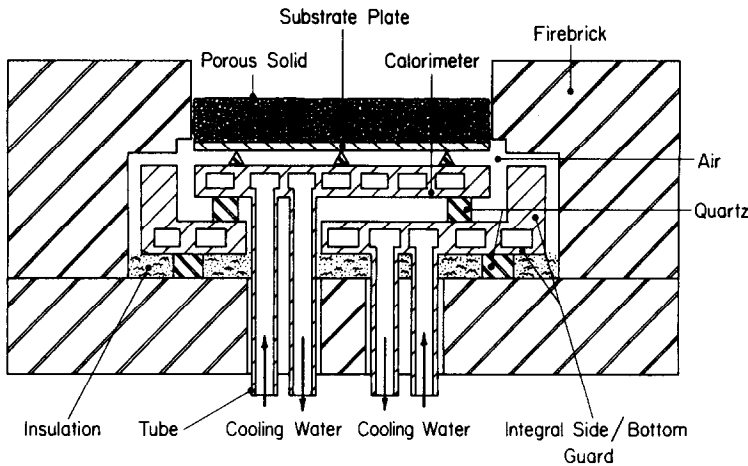


FIG. 1. Schematic of the test cell used to measure overall thermal conductances of porous solids.

and to protect the guard from the furnace environment. Chromel–alumel thermocouples were used to measure the temperatures of the heated and cooled surfaces of the porous solid. Copper–constantan thermocouples were employed elsewhere.

The one-dimensionality of heat transfer through the sample was confirmed by inspecting the uniformity of temperatures indicated by independent thermocouples at equivalent elevations. Readings for the lower surface of the sample differed by less than 4°C while those at the surface differed by less than 7°C. Since the temperature difference across a sample exceeded 180°C, heat transfer through the sample was considered to be one-dimensional.

The performance of the test cell was assessed by measuring the overall thermal conductances of two porous solid insulations and comparing the results with those obtained in accordance with ASTM-approved procedures [1]. Observed differences were within the 14% uncertainty of the experiments. Measurements were reproducible to within 3%.

## 2.2. Procedure and data reduction

Porous solids of known thicknesses were placed in the test cell, and thermocouple probes were installed at the top and bottom of the samples. Furnace temperatures between 400° and 1250°C were main-

tained. The flow rate of water to the calorimeter was adjusted to provide a coolant temperature rise of sufficient magnitude to reduce measurement error, while minimizing temperature gradients on the calorimeter surface. The flow rate to the integral guard was adjusted until its sidewall temperature equalled the temperature of the calorimeter.

All measurements were made at steady-state conditions, taken in seven batches, and averaged. Steady-state was presumed to have been reached when the temperature of the cooled surface of the sample changed by less than 0.2°C in a 15-min period. Overall thermal conductances were calculated from the measured heat rate, sample temperature difference, and sample thickness.

## 2.3. Materials studied

Five commercially available porous solids with uniform characteristics were selected and studied in six experiments. The fluid in the pores was air at atmospheric pressure. The compositions and porosities of each solid are given in Table 1. The first porous solid was a medium density firebrick which contains irregularly distributed and shaped pores that lie between splinter-like fragments of solid. It is composed principally of alumina and silica. All pores are less than about 1.5 mm in diameter and the porosity is 66%. The

Table 1. Compositions and porosities of selected porous solids

Porous solid	Experiment No.	$p$ (%)	Composition (% by weight)				
			Al <sub>2</sub> O <sub>3</sub>	SiO <sub>2</sub>	MgO	ZrO <sub>2</sub>	Other
Firebrick [16]	1	66	46.0	52.0	0.1	0.0	1.9
Alumina insulation [17]	2	85	83.0	17.0	0.0	0.0	0.0
Zirconia insulation [18]	3,4	92	0.0	0.0	0.0	91.5	8.5
Ceramic foams [19]	5	86	35.0	51.0	14.0	0.0	0.0
	6	88					

second porous solid was an insulating board which is composed mostly of alumina. It has a porosity of 85% and contains irregularly distributed and shaped pores that are formed between slightly sintered fibres which are 4–6  $\mu\text{m}$  in diameter. Unlike the firebrick, the pores are nearly uniform in size and range from 0.020 to 0.024 mm in average diameter. The third porous solid was an insulating board with a physical structure similar to that of the alumina insulation. However, it is unique in that its porosity is 92% and it is composed mostly of zirconia. Two samples of this insulation were tested with different thicknesses.

Unlike the other solids, which contain pores that are mostly enclosed by solid, the fourth porous solid was a ceramic foam in which the pores are interconnected and formed between an open skeletal structure. It is intended for use as a filtration medium at temperatures as high as 1150°C and is composed of cordierite ( $2\text{MgO} \cdot 2\text{Al}_2\text{O}_3 \cdot 5\text{SiO}_2$ ). It has a porosity of 86% and all pores have nearly identical geometries and are 0.73 mm in diameter. The fifth porous solid was a similar ceramic foam with a porosity of 88% and with pores that are 1.25 mm in diameter. The geometries of the pores in both ceramic foams are nearly identical.

### 3. THERMAL CONDUCTANCE MODEL

#### 3.1. Assumptions

The thermal conductance of a porous solid generally depends on physical parameters such as pore size, pore geometry and porosity, as well as on properties such as the thermal conductivities of the solid and fluid in the pores, and the emittance and transmittance of the solid. Conduction, convection and radiation may all contribute to the transport of heat. However, for the solids of this study, the characteristic size of the pores is sufficiently small to ensure that natural convection effects are negligible. Assuming a maximum tempera-

ture gradient of 750°C  $\text{cm}^{-1}$ , Rayleigh numbers remain less than 100 in pores as large as 10 mm.

Unit cell models which consider the material as opaque, the pore surfaces as gray and the pore gas as radiatively nonparticipating have successfully predicted thermal conductances for porous materials composed of firebrick particles, cement clinker, porcelain packing and iron spheres [12], as well as alumina ( $\text{Al}_2\text{O}_3$ ), zirconia ( $\text{ZrO}_2$ ) and magnesium oxide ( $\text{MgO}$ ) [13]. The simplicity and demonstrated success of these formulations for radiation heat transfer suggest their applicability to this model. In addition, conduction across the fluid in the pores is accounted for by introducing a dimensionless parameter  $\phi$ , which is the ratio of the effective length for conduction across a characteristic pore to the characteristic pore size. Yagi and Kunii [12] successfully applied such a parameter to predict conduction in voids of a packed bed and established its dependence on porosity, void geometry and fluid thermal conductivity.

Since the physical structures of many porous solids are complex, the thermal conductance model of this study uses characteristic geometric parameters to probabilistically define a unit cell for which an overall thermal resistance can be formulated from individual heat transfer mechanisms. This feature restricts applicability of the model to samples which contain a statistically significant number of pores. The average size of the pores must be small relative to the overall thickness of the sample, and the geometry and physical dimensions must not vary with temperature. Since many porous solids commonly have low thermal coefficients of expansion, variation of the geometry and dimensions with temperature can be neglected.

The assumptions used in the model are: (1) A solid with randomly distributed pores of complex geometry can be idealized as a structure in which all pores have a single characteristic size, are evenly spaced, and are randomly oriented with respect to their neighbors only

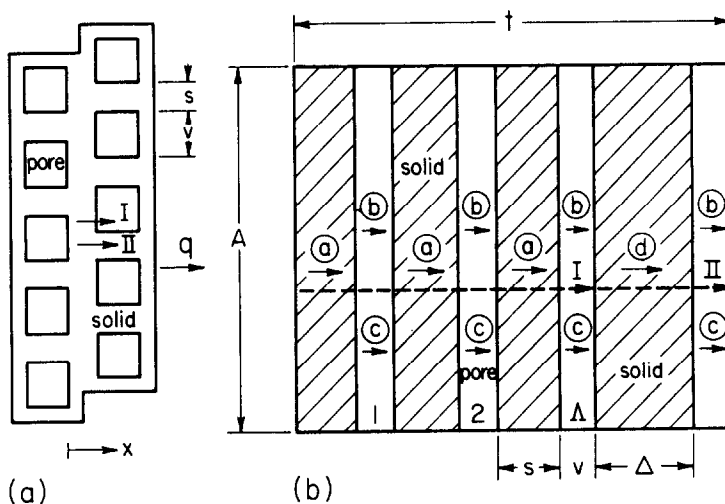


FIG. 2. Characteristic geometry (a) and equivalent unit cell (b) for thermal conductance model.

in the direction of heat flow [Fig. 2(a)]. (2) Conduction across the fluid in pores can be related to the characteristic size of the pores by the parameter  $\phi$ . (3) Heat transfer by thermal radiation occurs only across pores. The pore surfaces are gray diffuse emitters and reflectors, and the fluid in the pores is radiatively nonparticipating. The solid is opaque. (4) The geometry and dimensions of the material do not depend on temperature. (5) Heat transfer is one-dimensional.

### 3.2. Model formulation

The characteristic geometry for the porous solid model is shown in Fig. 2(a). In the model, the pore size,  $v$ , and the pore spacing,  $s$ , are uniform along the direction of heat flow and in the direction perpendicular to heat flow. The pore orientation in each successive column in the direction of heat flow is random. Two distinct paths for heat flow can be identified along a line drawn in the direction of heat flow beginning from the surface of a pore. Along path I, a part of every pore in some number of successive columns of pores is traversed; while for path II only one pore is encountered after passing through some distance of solid. Paths I and II are the only unique paths and occur in series since neither can begin unless preceded by the other.

An expectation value for the number of pores traversed by path I can be determined statistically. The probability of encountering a pore between successive rows of pores along the direction of heat flow can be expressed as  $\mu = v/(s+v) = \beta/(1+\beta)$ , where  $\beta$  is the ratio of the characteristic pore size,  $v$ , to the characteristic pore spacing,  $s$ . The number of pores contained in a distance  $x$  is then  $N = x/(s+v) = \mu x/v$ , and the probability of traversing  $N$  pores in succession along  $x$  is  $(\mu)^{\mu x/v}$ .

If, on average, the number of pores contained in path I is given by  $\Lambda$ , the expectation length of path I can be expressed as

$$\Lambda(s+v) = \int_{s+v}^{\infty} x(\mu)^{\mu x/v} dx \Big/ \int_{s+v}^{\infty} (\mu)^{\mu x/v} dx \quad (1)$$

from which it follows that

$$\Lambda = 1 + \left( \ln \frac{\beta+1}{\beta} \right)^{-1} \quad (2)$$

An effective length  $\Delta$  for conduction through the solid along path II can be similarly determined. If  $\gamma = 1 - \mu$  is the probability of not encountering a pore between successive columns of pores along the direction of heat flow, the probability of not encountering a pore along the distance  $x$  is  $\gamma^N = \gamma^{\mu x/v}$  from which it follows that

$$\Delta = \frac{\int_{2s+v}^{\infty} x \gamma^{\mu x/v} dx}{\int_{2s+v}^{\infty} \gamma^{\mu x/v} dx} = \frac{v(1+\beta) \left[ \frac{2+\beta}{1+\beta} \ln(1+\beta) + 1 \right]}{\beta \ln(1+\beta)} \quad (3)$$

In terms of the characteristic geometry in Fig. 2,  $\beta$  is related to the porosity  $p$  by

$$\beta = \frac{p^{1/3}}{1-p^{1/3}} \quad (4)$$

An effective unit cell which incorporates heat transfer paths I and II is represented in Fig. 2(b) in terms of the parameters  $\Lambda$ ,  $\Delta$ ,  $v$  and  $s$ . The heat transfer mechanisms are: (a) conduction through solid along path I; (b) conduction across fluid in a pore along paths I or II; (c) radiation heat transfer across pores in path I and across the pore of path II; and (d) conduction through solid of path II. Heat transfer mechanisms (a) and (d) occur in series with mechanisms (b) and (c), which are in parallel.

The length of the equivalent unit cell is  $\Lambda(s+v) + \Delta + v$ . The number of equivalent unit cells contained in a length  $t$  is thereby

$$\eta = t/v \left[ \Lambda \left( \frac{\beta+1}{\beta} \right) + \frac{\Delta}{v} + 1 \right] \quad (5)$$

The thermal resistance associated with the length  $t$  is  $R_t = \eta(R_I + R_{II})$ , where

$$R_I = \frac{\Lambda}{A} \left[ \frac{s}{k_s} + \frac{1}{h_{rv} + (k_r/\phi v)} \right] \quad (6)$$

and

$$R_{II} = \frac{1}{A} \left[ \frac{\Delta}{k_s} + \frac{1}{h_{rv} + (k_r/\phi v)} \right] \quad (7)$$

The local thermal conductance,  $K$ , of a porous solid of thickness,  $t$ , is related to  $R_t$  by  $K = t/AR_t$ . Using the expressions for  $\Lambda$ ,  $\Delta$ ,  $\beta$  and  $\eta$ , the local thermal conductance can be expressed as

$$K = \left[ \zeta + \Lambda \left( \frac{\beta+1}{\beta} \right) + 1 \right] \left[ \frac{1}{k_s} \left( \frac{\Lambda \psi}{\beta} + \zeta \right) + (1+\Lambda) \left( v h_{rv} + \frac{k_r}{\phi} \right)^{-1} \right]^{-1} \quad (8)$$

where

$$\zeta = \frac{\Delta}{v} = \frac{(1+\beta) \left[ \left( \frac{2+\beta}{1+\beta} \right) \ln(1+\beta) + 1 \right]}{\beta \ln(1+\beta)} \quad (9)$$

and  $\psi = 1$  for porous solids which have closed pores or  $\psi = 0$  for porous solids which have open pores. The parameter  $\phi$  can be determined by selecting the value which gives the best agreement between overall thermal conductances predicted with the model and those obtained experimentally at temperatures for which radiation is unimportant. (Values have been determined to range from approx. 0.3 to 0.7 for the porous solids of this study.) Note that  $K$  may not depend strongly on  $\phi$  if heat transfer across the pores occurs primarily by radiation.

The heat transfer 'coefficient' for thermal radiation across the pores can be formulated [5, 6] as

$$h_{rv} = 4\epsilon\sigma T^3 \quad (10)$$

where  $T$  is the average temperature of the pore surface.

In many porous solids, it is difficult to measure a discrete value for the characteristic pore size,  $v$ . For such cases,  $v$  may be found by adjusting its value until model predictions and experimentally determined thermal conductances agree at temperatures for which radiation is significant. Similarly, if the total hemispherical emissivity of the solid is unknown and does not change appreciably with temperature, the product  $v\epsilon$ , rather than  $v$ , can be adjusted.

The expression for local thermal conductance given by equation (8) is applicable to all porosities for solids which contain randomly oriented pores in statistically significant numbers. The parameters  $\Lambda$  and  $\zeta$  determine the relative importance of heat transfer paths I and II, respectively. The equivalent unit cell is thereby adaptable to suit a particular material porosity.

### 3.3. Determination of overall thermal conductance

The overall thermal conductance of a porous solid is defined as

$$k_e = \frac{q}{(T_H - T_C)/L} \quad (11)$$

Since heat transfer through a porous solid remains unchanged in the absence of internal heat generation, the temperature distribution is governed by the one-dimensional energy equation,

$$\frac{d}{dx} \left( K \frac{dT}{dx} \right) = 0 \quad (12)$$

This equation was solved numerically by successive over-relaxation [14] for stipulated values of  $T_H$ ,  $T_C$  and  $L$ , with values of  $K$  determined from the unit cell model, equation (8). The heat flux,  $q$ , was calculated from the temperature and local thermal conductance distributions using the Fourier–Biot law. With the heat flux known, equation (11) was used to calculate overall thermal conductance.

## 4. RESULTS AND DISCUSSION

### 4.1. Influence of significant parameters

4.1.1. *Effect of thickness and overall temperature difference.* In terms of the dimensionless variables  $\theta$  and  $\xi$ , the heat flux through a porous solid may be expressed in terms of the local and overall thermal conductances as

$$q = k_e \left( \frac{T_H - T_C}{L} \right) = \left( \frac{T_H - T_C}{L} \right) K \frac{d\theta}{d\xi} \quad (13)$$

from which

$$k_e = K \frac{d\theta}{d\xi} \quad (14)$$

For a particular porous geometry, the local thermal conductance  $K$  in equation (8) depends only on temperature, and equation (12) can be expressed in terms of the dimensionless variables  $\theta$  and  $\xi$  as

$$\frac{dK(\theta)}{d\theta} \left( \frac{d\theta}{d\xi} \right)^2 + K(\theta) \frac{d^2\theta}{d\xi^2} = 0 \quad (15)$$

The solution for  $\theta$  depends only on  $\xi$ . Hence, results for  $\theta(\xi)$  and  $K(\theta)$  are independent of  $L$  for identical values of heated and cooled surface temperatures. It follows from equation (14) that the overall thermal conductance is independent of the thickness  $L$ . Overall thermal conductances for packed beds were also found to be characterized by this behavior [15].

As the temperature difference  $T_H - T_C$  increases while the average temperature,  $T_{ave} = (T_H + T_C)/2$ , remains constant,  $k_e$  increases. This behavior is due to radiation effects which, from equation (10), vary as the third power of the local temperature. Moreover, unlike results for which only thickness is varied, the temperature profiles are not similar, as shown in Fig. 3, since local thermal conductances become higher at the heated surface and lower at the cooled surface as the temperature difference is increased.

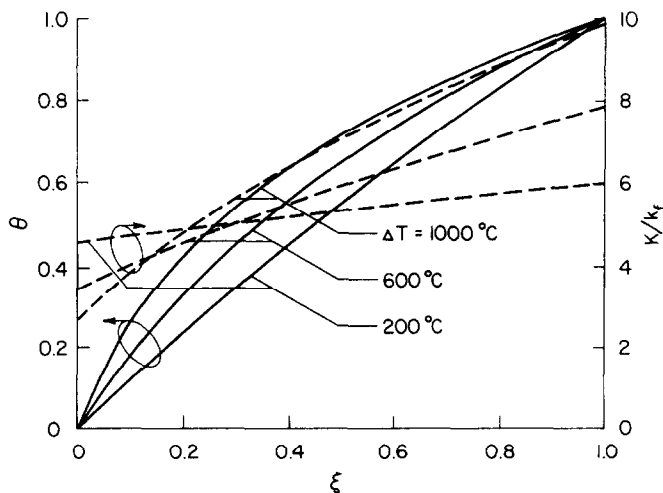


FIG. 3. Temperature and thermal conductance profiles for the alumina insulation at various overall temperature differences:  $v = 2.5$  mm,  $p = 85\%$ ,  $\phi = 0.563$ ,  $\psi = 1$ ,  $T_{ave} = 700^\circ\text{C}$ .

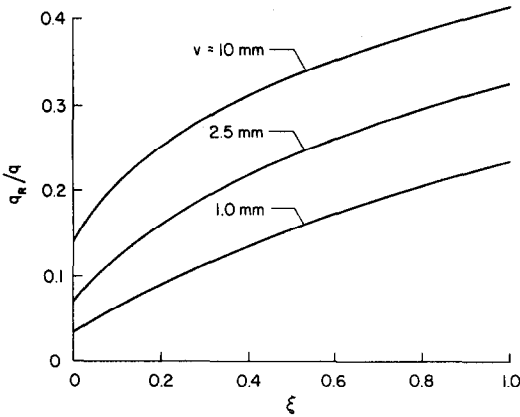


FIG. 4. Contribution of radiation to total heat transfer for various pore sizes in the alumina insulation:  $p = 85\%$ ,  $\phi = 0.563$ ,  $\psi = 1$ ,  $T_C = 400^\circ\text{C}$ ,  $T_H = 1000^\circ\text{C}$ .

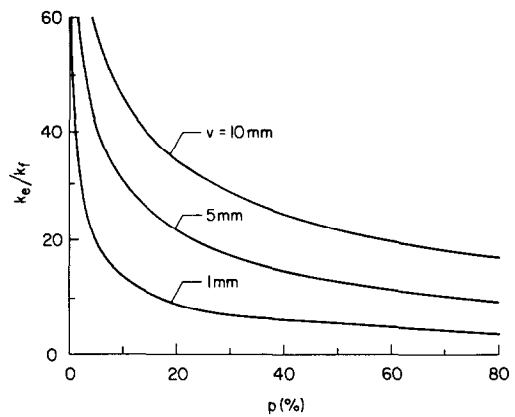


FIG. 6. Effect of porosity on overall thermal conductance in the alumina insulation for different pore sizes:  $\phi = 0.563$ ,  $\psi = 1$ ,  $T_C = 400^\circ\text{C}$ ,  $T_H = 1000^\circ\text{C}$ .

4.1.2. *Effect of pore size and porosity.* Since radiative transport occurs only between the surfaces of pores in an opaque porous solid, heat transfer is enhanced by increasing pore size for a fixed pore geometry and overall thermal conductance varies linearly with pore size. The effect of pore size on the radiation heat flux is shown in Fig. 4.

As the porosity of a solid with uniform pore size increases, heat transfer through the solid around the pore (path II in Fig. 2) diminishes. A larger fraction of the total heat transfer must be accommodated by conduction through the fluid in the pores and by thermal radiation. If thermal radiation is significant, local and overall thermal conductances can increase with increasing porosity. Figure 5 illustrates the influence of temperature, pore size and porosity on local thermal conductance in the manner of Chiew and Glandt [9]. For many porous solids, the parameter  $v$  of Fig. 5 remains less than unity and overall thermal conductance decreases with increasing porosity. This effect is shown in Fig. 6 for different pore sizes. Francl and Kingery [4] measured overall thermal conductances for alumina samples in which cylindrical holes

(0.82 mm) were drilled and found a porosity dependence similar to that of Fig. 6.

4.2. *Experimental results and model predictions*

The overall thermal conductance of a firebrick sample was measured in the first experiment and results are given in Fig. 7. Upon adjustment of the parameter  $\phi$ , model predictions agreed well with experimental values. Although visual examination revealed an average pore size of less than 1.5 mm, the precise size of the pores could not be determined due to their complex geometry. The pore size,  $v$ , was adjusted to 0.29 mm to provide best agreement with the data. The overall thermal conductances from the experiments were less than those provided in ref. [16], which were measured in accordance with ASTM procedures. Disparities are attributed to differences between the test cell designs which induced unique temperature differences for the

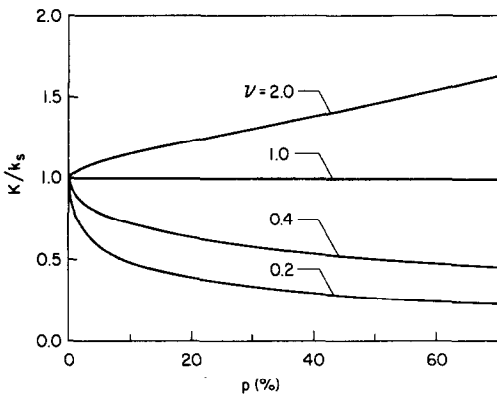


FIG. 5. Dependence of local thermal conductance on porosity for different temperatures and pore sizes:  $k_r = 0$ ,  $k_s = 7 \text{ W m}^{-1} \text{ K}^{-1}$ .

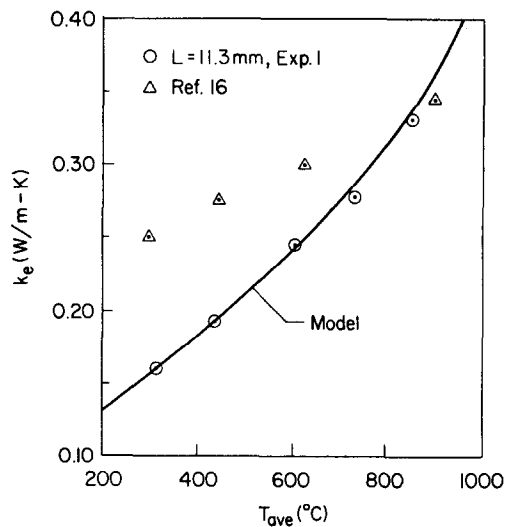


FIG. 7. Comparison of measured and predicted overall thermal conductances for firebrick:  $p = 66\%$ ,  $\phi = 0.406$ ,  $v = 0.29$  mm,  $\psi = 1$ .

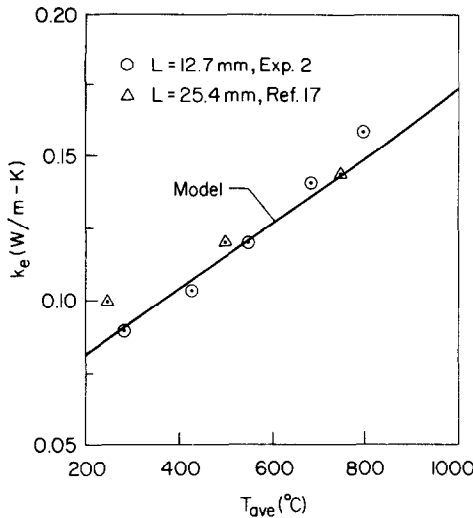


FIG. 8. Comparison of measured and predicted overall thermal conductances for the alumina insulation:  $p = 85\%$ ,  $\phi = 0.563$ ,  $v = 0.022$  mm,  $\psi = 1$ .

same average temperature and to physical variations amongst firebrick batches.

In the second experiment, overall thermal conductances for alumina insulation, 12.7 mm thick, were measured and found to agree well with those of ref. [17]; see Fig. 8. Also, with  $\phi$  set equal to 0.563, model predictions agreed well with experimental values.

Zirconia insulation was tested in the third and fourth experiments, and the results are given in Fig. 9. The sample thicknesses were 10.9 and 5.7 mm in the third and fourth experiments, respectively. To within the uncertainty of the experiments, the overall thermal conductances were equivalent and in agreement with the results of ref. [18] for samples of greater thickness (about 25 mm). The value of  $\phi$  was determined for

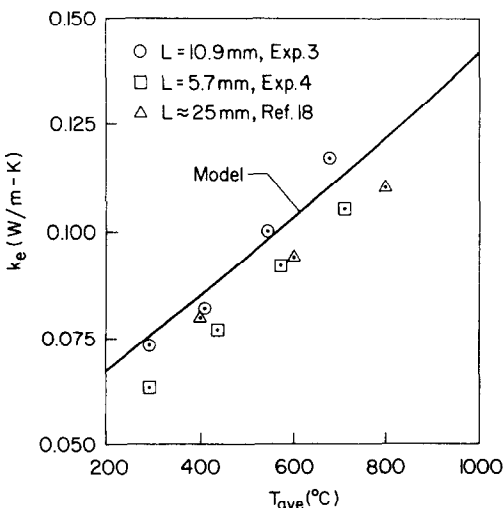


FIG. 9. Comparison of measured and predicted overall thermal conductances for the zirconia insulation:  $p = 92\%$ ,  $\phi = 0.645$ ,  $v = 0.0022$  mm,  $\psi = 1$ .

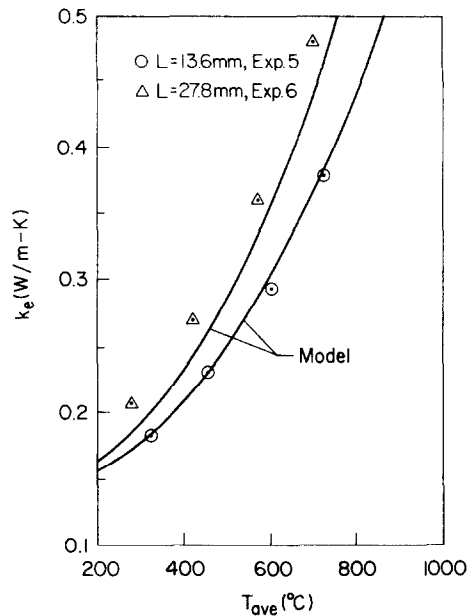


FIG. 10. Comparison of measured and predicted overall thermal conductances for ceramic foam filtration media. Experiment 5:  $L = 13.6$  mm,  $p = 86\%$ ,  $\phi = 0.313$ ,  $v = 0.73$  mm,  $\psi = 0$ . Experiment 6:  $L = 27.8$  mm,  $p = 88\%$ ,  $\phi = 0.313$ ,  $v = 1.25$  mm,  $\psi = 0$ .

Experiment 3 and was used to predict the overall thermal conductances of Experiment 4. Model-generated overall thermal conductances were nearly identical for both experiments. Small differences were due to minor disparities in the overall temperature differences, owing to the different thicknesses.

In Experiments 5 and 6, respectively, 13.6- and 27.8-mm samples of ceramic foam with  $v = 0.73$  and 1.25 mm were tested. As shown in Fig. 10, the overall thermal conductance is higher for the sample with the larger pores, but differences are smaller at lower average temperatures for which radiation is less significant. The value of  $\phi$  was determined for Experiment 5 and used to predict overall thermal conductances of Experiment 6. Since the pores in the ceramic foams are interconnected such that solid is not present between pores, a value of zero was used for  $\psi$ . The model predictions in both cases agree with measured values to within the uncertainty of the experiments. Since the geometries of both materials are nearly identical, the experiments indicate that the parameter  $\phi$  is not strongly dependent on the size of the pores. In addition, the heat transfer coefficient for radiation given by equation (10) provides good results, even though the pores are interconnected.

## 5. CONCLUSIONS

Agreement between experimental and model-generated results suggests that the thermal conductance model, for which a unit cell is treated probabilistically, the solid is gray and opaque, and the



fluid is radiatively nonparticipating, adequately represents several porous solids. Overall thermal conductance increases with increasing overall temperature difference and average temperature. As the temperature difference increases, the contribution to heat flow by radiation becomes larger. In materials where radiation is important, overall thermal conductances should be correlated to both average temperature and temperature difference. Overall thermal conductance does not depend on thickness when the thickness is much larger than the characteristic size of the pores. Thermal conductance increases with increasing pore size since the distance across which radiation can propagate becomes greater. Overall thermal conductance can increase or decrease with increasing porosity, depending on the importance of radiation.

*Acknowledgements*—This work was supported, in part, by the U.S. Department of Energy under Grant DE-FE22-81PC40789 and by the Coal Research Center of Purdue University.

#### REFERENCES

1. American Society for Testing and Materials, *1983 Annual Book of ASTM Standards, Part 17, Refractories, Glass, Ceramic Materials; Carbon and Graphite Products*, American Society for Testing and Materials, Philadelphia, PA (1983).
2. M. Hollingsworth, Jr., Experimental determination of the thickness effect in glass fiber building insulation, *Thermal Insulation Performance*, ASTM STP 718, pp. 255–271. American Society for Testing and Materials, Philadelphia, PA (1983).
3. C. J. Shirliffe, Effect of thickness on the thermal properties of thick specimens of low density thermal insulation, *Thermal Insulation Performance*, ASTM STP 718, pp. 36–50. American Society for Testing and Materials, Philadelphia, PA (1980).
4. J. Franci and W. D. Kingery, Thermal conductivity: IX. Experimental investigation of effect of porosity on thermal conductivity, *J. Am. ceram. Soc.* **37**, 99–100 (1954).
5. A. L. Loeb, Thermal conductivity: VIII. A theory of thermal conductivity of porous materials, *J. Am. ceram. Soc.* **37**, 96–99 (1954).
6. T. Saegusa, K. Kamata, Y. Iida and N. Wakao, Thermal conductivities of porous solids, *Heat Transfer-Jap. Res.* **3**, 47–52 (1974).
7. S. Whitaker, Radiant energy transport in porous media, *Ind. Engng Chem. Fundam.* **19**, 210–218 (1980).
8. J. C. Maxwell, *A Treatise on Electricity and Magnetism*, 2nd edn., Vol. I. Clarendon Press, Oxford (1881).
9. Y. Chiew and E. Glandt, Simultaneous conduction and radiation in porous and composite materials: effective thermal conductivity, *Ind. Engng Chem. Fundam.* **22**, 276–282 (1983).
10. J. C. R. Turner, The electrical conductance of liquid-fluidized beds of spheres, *Chem. Engng Sci.* **31**, 487 (1976).
11. G. D. Fetters, R. Viskanta and F. P. Incropera, Experimental study of heat transfer through coal ash deposits, ASME Paper No. 82-WA/HT-30 (1982).
12. S. Yagi and D. Kunii, Studies on effective thermal conductivities in packed beds, *Am. Inst. chem. Eng. J.* **3**, 373–381 (1957).
13. A. V. Luikov, A. E. Shashkov, L. L. Vasiliev and Yu. E. Fraiman, Thermal conductivity of porous systems, *Int. J. Heat Mass Transfer* **11**, 117–140 (1968).
14. S. V. Patankar, *Numerical Heat Transfer and Fluid Flow*, pp. 67–68. McGraw-Hill, New York (1980).
15. D. A. Zumbunnen, R. Viskanta and F. P. Incropera, Heat transfer through granular beds at high temperature, *Wärme-u. Stoffübertr.* **18**, 221–226 (1984).
16. Product Information for Type K-28 Insulating Firebrick, Babcock & Wilcox, Insulating Products Division, Augusta, Georgia, U.S.A. (May 1978).
17. Product Information for Alumina Insulating Board Type AL-30, Zircar Products, Inc., Florida, New York, U.S.A. (February 1981).
18. Product Information for Zirconia Insulating Board Type ZYFB3, Zircar Products, Inc., Florida, New York, U.S.A. (November 1978).
19. Bridgestone Ceramic Foam, Technical Report No. 1, Bridgestone Tire Co., Ltd., Tokyo, Japan (1984).

#### TRANSFERT THERMIQUE DANS LES SOLIDES POREUX AVEC DES GEOMETRIES INTERNES COMPLEXES

**Résumé**—On développe un modèle de conductance thermique pour le transfert thermique dans un solide poreux, en utilisant une cellule unitaire déterminée par voie probabiliste pour une géométrie caractéristique. On réalise un appareil pour mesurer les conductances thermiques globales (conductivités thermiques effectives) de plusieurs solides poreux dans un large domaine de température. Un paramètre nécessité par le modèle est inféré à partir des mesures, et les conductances thermiques calculées et mesurées s'accordent dans le cadre des imprécisions des expériences. Des calculs paramétriques montrent que, quand le rayonnement est significatif, la conductance thermique globale augmente avec la différence de température à travers le solide poreux et qu'elle est indépendante de l'épaisseur quand celle-ci est grande par rapport à la taille des pores.

#### WÄRMEÜBERTRAGUNG IN PORÖSEN FESTSTOFFEN MIT KOMPLIZIERTER INNERER GEOMETRIE

**Zusammenfassung**—Es wurde ein Modell für die Wärmeübertragung in porösen Feststoffen unter Verwendung einer wahrscheinlichkeitstheoretisch ermittelten Einheitszelle als charakteristische Geometrie entwickelt. Ein Gerät zur Messung der effektiven Wärmeleitfähigkeit von verschiedenen porösen Feststoffen in einem großen Temperaturbereich wurde konstruiert. Die Messungen ließen auf einen für das Modell notwendigen Parameter schließen; dieser wurde bestimmt. Die gemessenen effektiven Wärmeleitfähigkeiten stimmten innerhalb der Fehlergrenzen mit den berechneten überein. Parameterstudien weisen darauf hin, daß die effektive Wärmeleitfähigkeit mit der Temperaturdifferenz im porösen Feststoff ansteigt, solange der Strahlungseinfluß maßgebend ist, und unabhängig von der Dicke ist, solange das Verhältnis Dicke zu Porengröße groß ist.

## ТЕПЛОПЕРЕНОС В ПОРИСТЫХ ТВЕРДЫХ ТЕЛАХ СО СЛОЖНОЙ ВНУТРЕННЕЙ ГЕОМЕТРИЕЙ

**Аннотация**—Модель теплопроводности в пористом твердом теле получена с использованием элементарной ячейки, определенной вероятностным методом, для некоторой характерной геометрии. Разработано устройство, с помощью которого измерена суммарная эффективная теплопроводность нескольких пористых твердых тел в широком диапазоне температур. Параметры модели определены из экспериментов, а рассчитанные и измеренные значения суммарной теплопроводности согласуются между собой в пределах погрешности экспериментов. Параметрические расчеты свидетельствуют о том, что в случае существенной радиации суммарная теплопроводность растет с увеличением разности температур поперек пористого твердого тела и не зависит от толщины, когда последняя значительно превышает размер поры.